Detection of Visual-Data Transitions in "Nonlinear Parameter-Space"

Rainer Sprengel, Christoph Schnörr, Bernd Neumann

FBI-HH-M 235/94

December 1993

Arbeitsbereich Kognitive Systeme
FB Informatik, Universität Hamburg
Bodenstedtstr. 16, 2000 Hamburg 50, FRG

Zusammenfassung

Wir schlagen eine neue Methode zur Detektion von signifikanten Übergängen in verrauschten visuellen Daten vor. Die Methode basiert auf einem allgemein einsetzbaren, globalen Minimierungsansatz, der kürzlich als natürliche Erweiterung des quadratischen Variationsprinzips vorgeschlagen wurde, welches in der Bildverarbeitung oft zur Regularisierung schlecht gestellter Probleme eingesetzt wird. Dieser Ansatz erlaubt eine räumliche Integration visueller Daten, bei welcher signifikante Änderungen in den Daten erhalten bleiben, ohne, daß dabei auf die günstigen Eigenschaften quadratischer Minimierungsansätze verzichtet werden muß: Existenz, Eindeutigkeit und Stabilität der Lösung, sowie ihre stetige Abhängigkeit von den Daten.

In dieser Arbeit wird die Abhängigkeit der Lösung des Minimierungsproblems von den globalen Parametern analysiert, die den zugehörigen Diffusionsprozeß steuern. Die Ergebnisse motivieren eine neuartige Methode zur Detektion und Lokalisation von signifikanten Übergängen in verrauschten Daten. Es wird nach Punkten gesucht, die "stabil" bzgl. infinitesimal kleiner Änderungen an den globalen Parametern sind. Numerische Beispiele auf Daten natürlicher Szenen zeigen, daß diese Punkte zur Charakterisierung einer Reihe von typischen Übergängen dienen können.

Abstract

We present a novel scheme for the detection of transitions in noisy visual data. The scheme is based on a general global minimization approach that we have recently proposed as a natural extension of quadratic variational principles used in vision. This approach provides a transition-preserving spatial integration stage without loss of the advantageous properties of quadratic minimization problems: well-posedness, uniqueness, convergence and stability of numerical schemes.

In this paper, we analyze the dependence of nonlinearly smoothed functions on global parameters which control the associated diffusion process. The results motivate a novel definition for the detection of transition points in noisy data. The corresponding algorithm looks for points that are "stable" with respect to infinitesimal parameter perturbations. Numerical examples with real data show that these points provide a useful characterization of various types of transitions over scale.

Keywords: Variational regularization, nonlinear diffusion, piecewise smooth functions, data reduction, segmentation.

1 Introduction

1.1 Overview

The robust integration of local visual features into non-local coherent descriptions of images is an important task of low-level vision. Concerning the hierarchy of processing stages from raw pixel data towards higher cognitive functions, redundant data should be discarded as early as possible. In general, this amounts to locally correlating computed feature values (in space and time) with some smoothing or filtering operation. On the other hand, visual features indicating the structure of the surrounding scene must not be destroyed by the smoothing procedure. These conflicting demands are usually called the segmentation problem. As any processing stage, a solution to this problem should be based on a mathematical description making explicit (i) the mappings used to transform input data from both, bottom up and top down (feedback) pathways, to output data, and (ii) the computational architectures by which the corresponding processes can be carried out.

A wide range of smoothing schemes for integrating visual data, like greyvalues, motion, texture, etc., can be described by quadratic variational principles. Based on *a priori* knowledge about qualitative properties of the data, constraint terms can be specified to compute smooth global representations of the visual input by minimizing quadratic functionals. The mathematical characterization of this class of problems can be found in the literature [1], and efficient stable algorithms can be devised for conventional hardware [28] or analogue networks [20, 11]. Related biological models have been pointed out by [29].

A major drawback of quadratic variational approaches, however, is that important local clues with respect to the structure of the scene are wiped out by the smoothing process. Therefore, we have developed an extension of the quadratic variational principle that preserves significant variations of the input data and is applicable to a wide range of early vision tasks [22]. Furthermore, our approach inherits the attractive properties of the quadratic principle (see [23, 24] and Section 2), and thus appears to be an useful compromise between the simplicity of quadratic minimization problems and the mathematical (non)tractability as well as algorithmic complexity of more involved global minimization problems that have been proposed in the literature to overcome the "discontinuity" problem (cf. next section).

Numerical results show that our approach preserves significant transitions of input data. However, according to the mathematical conditions imposed, these transitions (i.e. edges, motion boundaries, etc.) are not represented by "thin" lines but as transition regions. For example, ramp-like transitions are preserved as ramps and not as a sequence

of step edges. Therefore, to mark appropriate points that represent transition regions, we consider the behaviour of nonlinearly diffused signals dependent on the variation of global parameters that control the diffusion process (Section 3). Based on this, we develop a novel criterion for the detection of transition points and investigate the behaviour of these points over scale (Section 4).

1.2 Related work

The quadratic minimization approach has been introduced to the vision community by Horn and Schunck [10], and then has been applied to various problems (e.g., [12, 28]). Later, this approach has been termed "regularization" [21, 2], due to the resemblance to a mathematical concept that, for example, is known in the context of deconvolution problems.

To overcome the limitations of this class of approaches with respect to the segmentation problem, many approaches have been proposed that may be classified as follows: Non-quadratic global minimization approaches, either continuously formulated or discrete, or nonlinear-diffusion approaches. We briefly sketch the features of these research directions and refer for a more thorough discussion to [22].

Discrete extensions of the quadratic variational principle are based on so-called line processes [9] which incorporate additional unknown variables into the cost function in order to label data transitions. The problem formulation then becomes inherently discrete: The variables to be determined do not longer represent some "continuous" function, the problem solution depends on the specific coordinate system used. To minimize the resulting complex cost functions one uses either annealing processes (which are very often impractical) or heuristically traces the solution path with respect to a one-parameter family of cost functions (e.g. [9, 14, 3, 8]).

A continuously formulated extension of quadratic minimization problems has been presented by Mumford and Shah [15]. These authors directly addressed the problem to determine a function that may have jumps across the boundaries of an unknown decomposition of the underlying domain. It can be shown that solutions to this difficult minimization problem exist in very general function spaces [7, 4]. However, it seems to be unknown how regular these solutions are and (consequently) there is no theory of how to numerically approximate such solutions (cf. [26]). Recently, Ambrosio and Tortorelli proposed a family of (slightly) simpler functionals that are related to the Mumford-Shah functional in a precise mathematical sense. Corresponding algorithms, however, are still developed by using ad-hoc rules [13, 16].

A third line of research has been initiated by Perona and Malik [19]. They proposed a nonlinear version of the heat-equation to adaptively filter images. However, a corre-

sponding mathematical model has not been developed. The approach is ill-posed and corresponding algorithms are unstable (cf. [17]). The same statements probably apply to the approach of Nordström [18], who avoided the time-stopping problem by modifying Perona and Malik's equation such that it can be related to a minimization problem. Existence of a solution has not been proved, and it is not clear how this approach can be modelled using the classical Sobelev-space theory. Recently, interesting work has been published in the mathematical literatur [5]. These researchers developed a mathematical basis for a modified Perona-Malik equation and, apart from the time-stopping problem, report good results. The relationship to our approach should be worked out in future investigations.

1.3 Organization of this paper

In the next section, we outline the general minimization principle that underlies our work. Next we present results about the parameter dependence of nonlinearly diffused functions (Section 3). In Section 4, a novel criterion for the detection of transition points is developed. Using real data, the behaviour of these points over scale is explored. We summarize the results and indicate further work in Section 5.

2 Nonlinear diffusion as a strictly convex minimization problem

In this section, we briefly sketch our basic approach to the spatial integration of visual data. For details we refer to [22, 24, 27].

Let $\Omega \subset \mathbb{R}^2$ be a piecewise smooth domain within the image plane, and $g \in L^2(\Omega; \mathbb{R}^n)$ the input data. g may be raw pixel data ($n = 1$), motion data ($n = 2$), or, in general, the function associated with the output of a set of n-dimensional feature processing units. Our approach to integrate this locally computed data is to find a function $u \in \mathcal{H}$ in a suitable function space $\mathcal{H}$ such that the functional

$$J(v) = \int_\Omega \Big\{ |v - g|^2 + \lambda(\nabla v) \Big\}\, dx \tag{1}$$

attains its minimum. Depending on the choice of the function $\lambda(\cdot)$, this problem may be well-posed and have a unique solution. Furthermore, approximate solutions can numerically be determined by computing the solutions u_h in discrete subspaces $\mathcal{H}_h \subset \mathcal{H}$, respectively. To this end, by using standard discretization methods [6], vanishing of the first variation of J is expressed as a set of nonlinear equations

$$< J'(u_h), v_h > \;=\; 0\,, \quad \forall\, v_h \in \mathcal{H}_h\,,$$

which can easily be solved for u_h. In contrast to ad-hoc discretizations, these discrete solutions converge towards the solution $u \in \mathcal{H}$ as the discretization parameter h goes to zero:

$$\|u - u_h\|_{\mathcal{H}} \to 0 \quad \text{as} \quad h \to 0 \, .$$

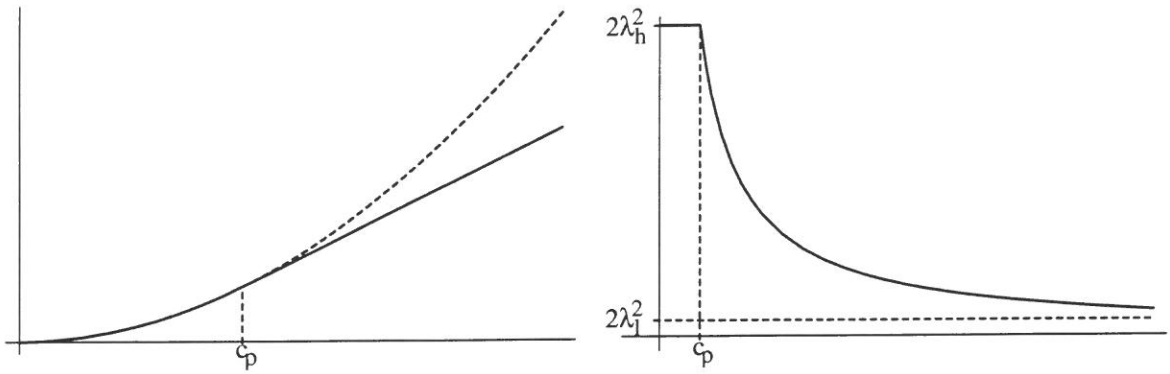

Figure 1: (a) $\lambda(t)$ (left) and (b) $\rho(t)$ (right)

Our choice of $\lambda(\cdot)$ depends on three (global) parameters, $\lambda(\cdot) = \lambda(\cdot; \lambda_h, \lambda_l, c_\rho)$, the meaning of which is illustrated in Figure 1. Figure 1b depicts the shape of the "diffusion"-coefficient ρ that is defined by the equation:

$$\lambda'(x) = \rho(|x|)x \, .$$

Figure 1 shows that, as soon as $|\nabla v|$ exceeds the value of c_ρ, the influence of the smoothness term in (1) decreases from λ_h to λ_l.

Alternatively, by setting the first variation of J to zero and subsequent partial integration, the minimizing function u may also be interpreted as the (weak) solution to the nonlinear diffusion equation

$$\frac{\partial v}{\partial t} = \nabla \cdot (\rho(|\nabla v|)\nabla v) + 2(g - v)$$

with Neumann condition at $\partial\Omega$.

3 Parameter-dependence of nonlinear diffused signals

In this section, we investigate the behaviour of solutions for our nonlinear diffusion process dependent on the variation of the global parameters λ_h, λ_l, and c_ρ (cf. Figure 1). The analysis presented in Section 3.1 shows (i) that λ_l is immaterial in this context and can be set to any small positive value (as a result, this reduces the number of effective parameters

to two), and (ii) that certain combinations of the remaining parameter λ_h and c_ρ are of primary importance.

These results are illustrated by numerical examples and are exploited for the detection of transition points investigated in Section 4.

3.1 Analytical results

In order to obtain analytical results, we have focused for the time being on the 1D-case. Our approach, however, does not depend on the dimensioning of the data, and we expect similar results to hold in the general case.

In the 1D-case, the diffusion equation reads:

$$g(x) = u(x) - u''(x) \begin{cases} \cdot\lambda_h^2 & \text{for} \quad |u'(x)| < c_\rho \\ \cdot\lambda_l^2 & \text{for} \quad |u'(x)| > c_\rho \end{cases} . \tag{2}$$

One of our goals is to derive the conditions for edge and ramp detection. To this end, we compute the solution of the linear diffusion equation with $\lambda = \lambda_h$ and compare the maximum gradient of this solution with the switching parameter c_ρ. We consider an edge or ramp as detected, if the gradient of the solution at this position is greater than c_ρ.

Closed-form solutions to (2) can be computed for various simple functions g: The Sobolev embedding theorem tells us that the solution u must be continuous. This gives the boundary conditions for each region corresponding to $u'(x)$ in (2), and thus u can be computed by convolving the data g with the associated Green-functions.

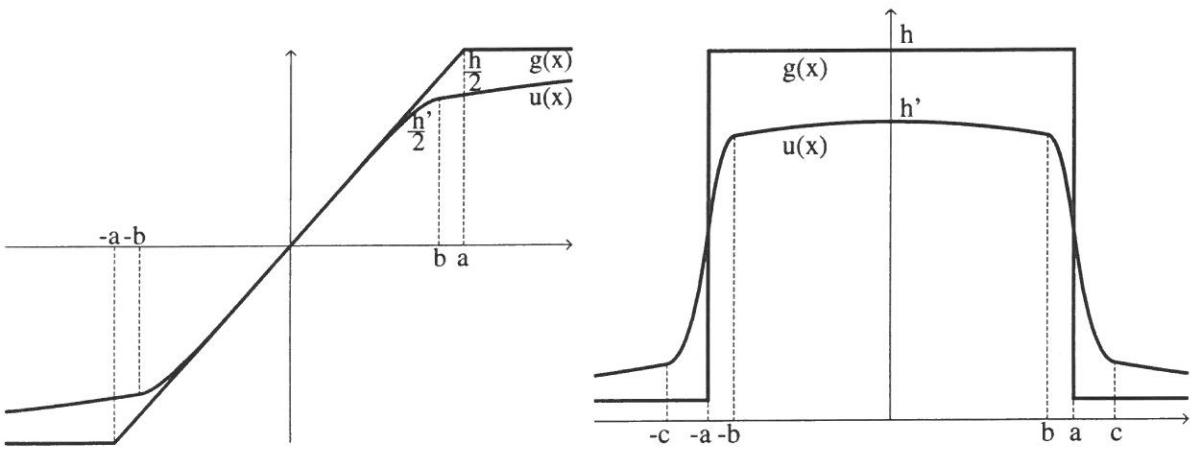

Figure 2: Ramp edge (left) and rectangle signal (right)

Table 1 shows the results computed for the isolated step edge (height h), the isolated ramp edge (width $2a$, height h, gradient $m = h/2a$; Figure 2), and a rectangular signal (width $2a$, height h; Figure 2). Figure 2 shows also a typical solution u with the switching points (at $x = b$ and $x = c$) which separate the low-smoothing from the high-smoothing regions.

	step edge	ramp edge	rectangle
linear energy	$\lambda h^2/2$	$m^2\lambda^2\left(2a - \lambda(1-e^{-\frac{2a}{\lambda}})\right)$	$h^2\lambda\left(1-e^{-\frac{2a}{\lambda}}\right)$
max. linear gradient	$\frac{h}{2\lambda}$	$\frac{h}{2a}(1-e^{-a/\lambda})$	$\frac{h}{2\lambda}(1-e^{-2a/\lambda})$
sensitivity threshold h_0	$h_0 = 2c_\rho\lambda_h$	$h_0 > 2c_\rho\lambda_h$, $a \ll \lambda_h$ $h_0 > 2ac_\rho$, $a \gg \lambda_h$	$h_0 > c_\rho\lambda_h^2/a$, $a \ll \lambda_h$ $h_0 > 2c_\rho\lambda_h$, $a \gg \lambda_h$
reconstructed height h'	$h' < h - 2c_\rho\lambda_h$	$h' < h - 2c_\rho\lambda_h$	$h' \approx h - c_\rho\lambda_h^2/a$
width of low-smoothing region	$\epsilon < \lambda_l \operatorname{acosh}(\frac{h}{c_\rho\lambda_h})$ $< \lambda_l\sqrt{2(\frac{h}{c_\rho\lambda_h}-1)}$	$\epsilon \approx \epsilon_{\text{step}}$, $m > c_\rho(1+\frac{\lambda_h}{\lambda_l})$ $\epsilon \approx a - \lambda_h\frac{c_\rho}{m}$, $c_\rho \ll m < c_\rho(1+\frac{\lambda_h}{\lambda_l})$	$\epsilon < \epsilon_{\text{step}}$

Table 1: Parameter dependence for various data g

From Table 1, the following observations can be made:

- The value $2c_\rho\lambda_h$ is a contrast sensitivity threshold determining the minimum contrast h_0 necessary for the detection of an isolated step or ramp edge. An edge is considered as isolated if there are no other features within a neighborhood which is large compared to λ_h. Thus, λ_h is a characteristic distance for the interaction of discontinuities (cf. [3]).

- The value of $c_\rho\lambda_h$ is also responsible for the height h' of the reconstructed signal. The height h' is defined as the difference between the two values of u at the switching points at both sides of the step or ramp (see Figure 2).

- A ramp edge can only be detected if its gradient is greater than c_ρ and if the ramp is wide enough. Note that a ramp is always reconstructed as a ramp. There is no limit of the gradient causing a ramp to split into several spurious step edges, as is the case for the weak string (or membrane) model of Blake and Zisserman [3].

- In the case of interacting steps ($a \ll \lambda_h$), the contrast sensitivity threshold increases by a factor $\lambda_h/2a$. Here, $c_\rho\lambda_h^2$ must be less than the area under the rectangle. The higher the steps, the closer they can be. The value of $c_\rho\lambda_h^2$ plays also a crucial role for the difference of the original and the reconstructed height (Figure 2, in the middle of the rectangle).

- Another interesting fact is that the difference of the maximal gradient of the nonlinear solution to the linear solution with $\lambda = \lambda_l$ is very small. Furthermore the value of λ_l has no effect on the detection properties and we can always choose some low value for this parameter.

3.2 Coping with noise

Consider a step function which is degraded by an additive white noise process. We want to derive some constraints on the parameters in order to detect the step edge while at the same time smoothing out the noise.

Let us first consider the case of linear diffusion of the data

$$g(x) = h(x) + n(x), \qquad n \sim \mathcal{N}(0, \sigma^2).$$

Here, $h(x)$ is the step function of height h. With the associated Green function $\Gamma(x, \xi)$ we can write the solution of this problem as a convolution of g with a linear filter G:

$$u(x) = \int_{-\infty}^{\infty} G(x - \xi) g(\xi)\, d\xi \qquad G(x - \xi) = \Gamma(x, \xi) = \frac{1}{2\lambda} e^{-\frac{|x-\xi|}{\lambda}}.$$

Additive white Gaussian noise of variance σ is transformd by a linear filter G into Gaussian noise with variance

$$\sigma_u^2 = \sigma^2 \int_{-\infty}^{\infty} G^2(t)\, dt = \frac{1}{4\lambda}.$$

For the gradient u' of the solution this means:

$$u'(x) = \int_{-\infty}^{\infty} \frac{\partial G(x - \xi)}{\partial x} h(\xi)\, d\xi + \int_{-\infty}^{\infty} \frac{\partial G(x - \xi)}{\partial x} n(\xi)\, d\xi$$

with

$$\sigma_{u'}^2 = \sigma^2 \int_{-\infty}^{\infty} \left(\frac{\partial G}{\partial x}(t) \right)^2 dt = \frac{\sigma^2}{4\lambda^3}$$

The solution to the linear diffusion equation is also the solution of our nonlinear diffusion equation (with $\lambda = \lambda_h$), as long as the maximum gradient of the solution does not exceed the switching parameter c_ρ. The maximum gradient of the linear solution for the ideal step of height h is

$$u'_{\max} = \max_{x \in \mathbb{R}} |u'(x)| = \frac{h}{2\lambda_h}.$$

In order to detect the step with high probability, we choose the value of c_ρ such that:

$$c_\rho \leq u'_{\max} - k\sigma_{u'} = \frac{h}{2\lambda_h} - \frac{k}{2} \frac{\sigma}{\lambda_h^{3/2}}.$$

$k = 2, 3$ are meaningful values. At the same time we have to choose c_ρ high enough in order not to detect steps that are due to noise only:

$$c_\rho \geq k\sigma_{u'} = \frac{k}{2} \frac{\sigma}{\lambda_h^{3/2}}.$$

For these constraints to be meaningful, λ has to satisfy

$$\lambda \geq \left(\frac{2k}{h/\sigma} \right)^2.$$

Thus, the higher the signal-to-noise ratio h/σ, the lower the smoothing parameter λ_h. Numerical examples illustrating this fact can be found in [24].

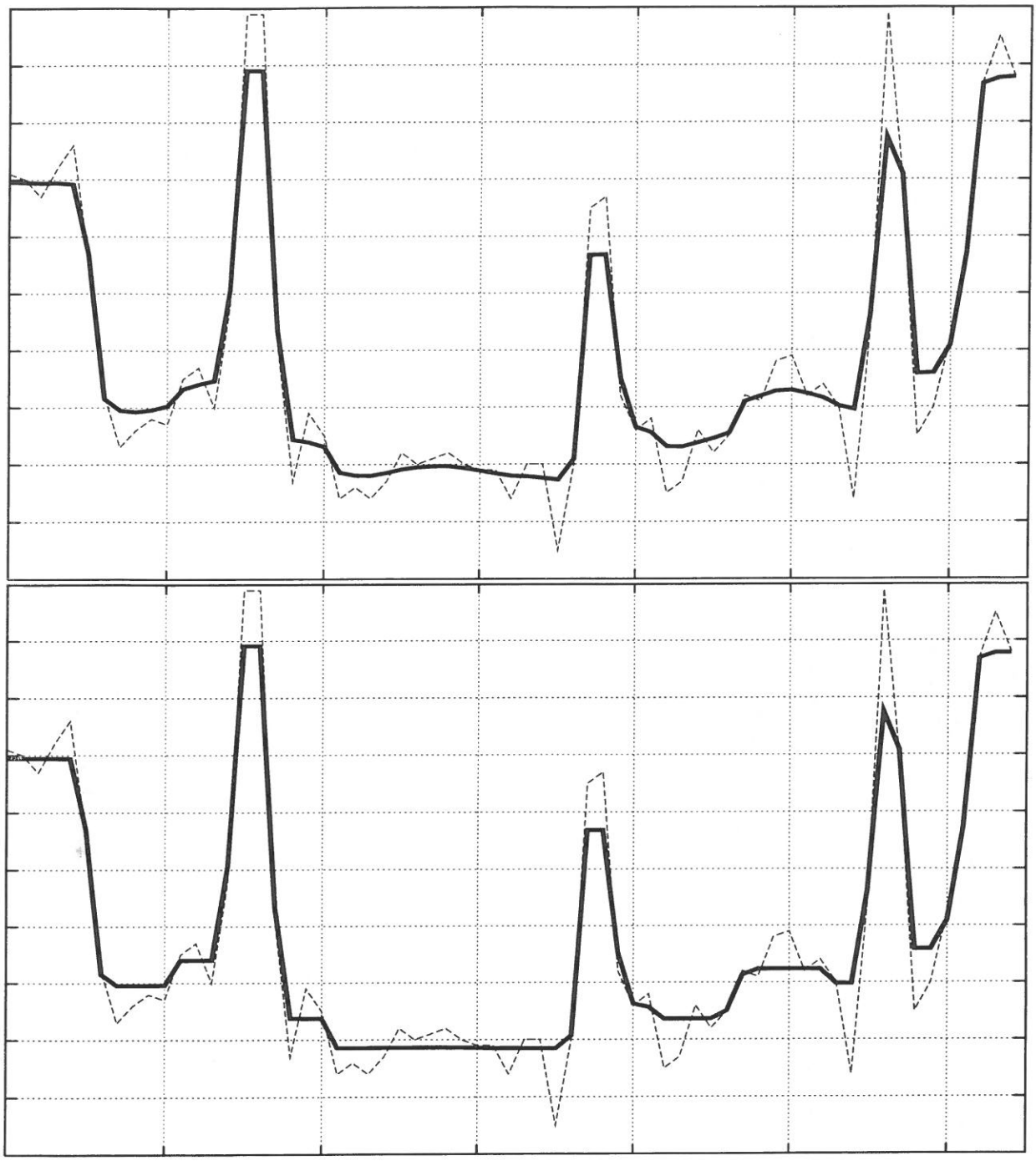

Figure 3: Result of nonlinear diffusion on real data (see Figure 4). Parameter values: $\lambda_h = 2.5, \lambda_l = 0.2, c_\rho = 1.0$ (top); $\lambda_h = 16, \lambda_l = 0.2, c_\rho = 0.024$ (bottom)

3.3 Discussion of analytical results using real data

In this paragraph we discuss some aspects of the analytical results of the previous subsections using real data. Figure 3 shows two results of nonlinear diffusion of the same data but with different parameter settings. Although we have chosen very different values for the high-smoothing parameter λ_h, we get very similar results because the value of $c_\rho \lambda_h^2$ is the same in both cases. Since the selectivity threshold and the reconstructed height for

interacting steps (see Table 1) is proportional to this combination of parameters we have no difference in the regions of thin peaks.

However, the value of $c_\rho \lambda_h$ in the first example (at the top of Figure 3) is higher than in the second. The low value of $c_\rho \lambda_h$ is the reason for the cornered shape of u in the second example. This can be explained by looking at the expressions for the reconstructed height in case of a step or ramp edge (Table 1). In case of a small value for $c_\rho \lambda_h$ we have a better approximation to a step function.

We conclude, that in order to segment a signal into several parts of nearly constant grey-value, we can choose a high value for the smoothing parameter λ_h as long as the corresponding value for the switching parameter c_ρ is low.

4 A novel approach to the detection of visual-data transitions

4.1 Definition of transition points

In the previous section we have shown, how the nonlinear diffusion process decomposes the underlying domain Ω into regions with high and low degree of smoothing, respectively. Regions where the algorithm has switched to the low-smoothing mode are indicated by $|\nabla u| > c_\rho$ (and vice versa). These are the regions where transitions of the data occur.

Figure 4 illustrates how the approach performs for real, noisy 2D-data. According to the mathematical conditions imposed (see Section 2), conservative estimates of transition regions are obtained (Figure 4, middle-right): the overall structure appears to be correct but the regions are broad. We consider this *not* as a drawback of our approach but as a consequence of the fact, that ramps are reconstructed as ramps, for example (see the discussion in Section 3.1).

For many applications, however, one wishes to represent transition-regions by curves within Ω. Our approach to mark points that are distinctive of the corresponding transition region goes as follows: For $c_\rho \to \infty$ the nonlinearity of our approach has no effect on the solution. Hence, slightly increasing c_ρ leads to an additional relaxation of the "tension" between hills and valleys of the data. It is intuitively clear that there exist boundaries between these regions that do not move during this relaxation process. Our approach is to represent transition regions by these boundaries that are obtained by infinitesimal variations of c_ρ.

Formally stated, we propose to look for zero-crossings of the tangent-vector of the curve in the function space $\mathcal{H}$ that is given by the family of nonlinearly diffused functions for varying c_ρ.

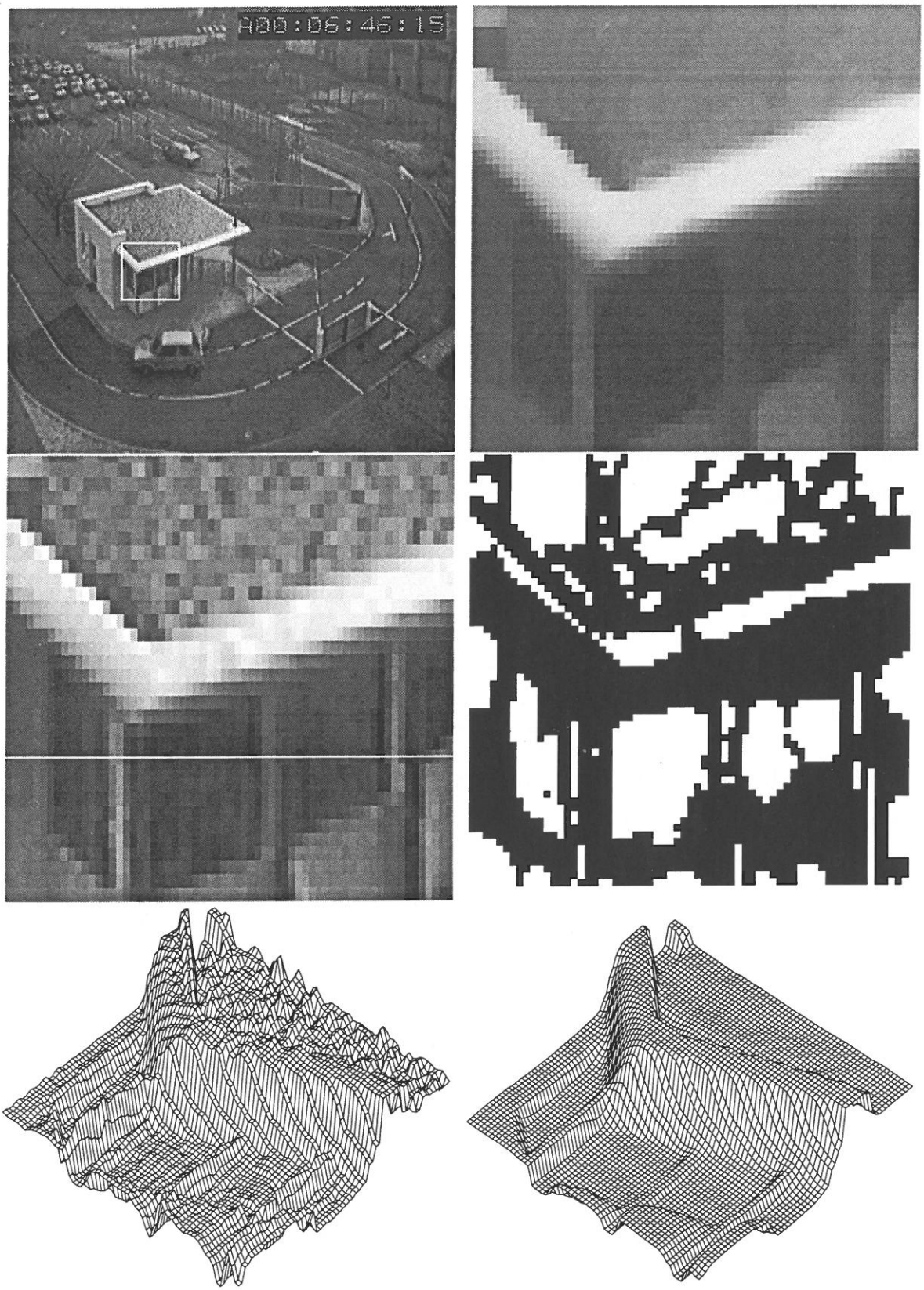

Figure 4: Section (middle-left) of an outdoor scene (top-left), result of 2-dimensional nonlinear diffusion with parameters $(\lambda_h, \lambda_l, c_\rho) = (7, 0.2, 0.4)$ (top-right) and the regions of low smoothing (middle-right). The original section and the result of nonlinear diffusion are plotted in the bottom pictures.

4.2 Computation of transition points

After discretization our minimization problem is described by a nonlinear system of equations: $F(u; c_\rho) = 0$. Taking the derivative with respect to the parameter c_ρ yields:

$$\frac{d}{dc_\rho} F(u(x; c_\rho); c_\rho) = \frac{\partial}{\partial u} F(u(x; c_\rho); c_\rho) \frac{d}{dc_\rho} u(x; c_\rho) + \frac{\partial}{\partial c_\rho} F(u; c_\rho) = 0.$$

Thus we have to solve the following system of linear equations in order to compute the derivative of the solution with respect to the parameter c_ρ:

$$u_{c_\rho} := \frac{d}{dc_\rho} u(x; c_\rho) = -\left(\nabla F(u)\right)^{-1} \frac{\partial}{\partial c_\rho} F(u; c_\rho).$$

In order to guarantee the differentiability of F we have to ensure that ρ is not only continuous but also differentiable. An appropriate and sufficiently close approximation preserving the mathematical properties of our approach ($\epsilon \ll c_\rho$) reads:

$$\rho(s) = \begin{cases} 2\lambda_h^2 & 0 \le s \le c_\rho \\ 2\lambda_l^2 + \lambda_\epsilon^2[2(c_\rho + \epsilon) - s - c_\rho^2/s] & c_\rho \le s \le c_\rho + \epsilon \\ 2\lambda_l^2 + \frac{\epsilon}{s}\lambda_\epsilon^2(\epsilon + 2c_\rho) & c_\rho + \epsilon \le s \end{cases}$$

with

$$\lambda_\epsilon^2 = \frac{\lambda_h^2 - \lambda_l^2}{\epsilon}.$$

It can be shown that ∇F is always a symmetric, positive definite matrix. In the one-dimensional case it is tri-diagonal, so that we can solve the system of equations with a direct numerical method [25]. It should be noted that this is a consequence of the mathematical properties of our approach to "nonlinear diffusion" described in Section 2.

4.3 Numerical examples and discussion

In this section, we show and discuss our approach by computing u_{c_ρ} for real image data. So far, we have made extensive numerical experiments for the 1D-case. The 2D- and 3D-case will be investigated in future work.

As data g we have taken the greyvalues of the row marked in Figure 4. This signal comprises several step and ramp like transitions, and thus is an appropriate candidate to test the performance of our approach over the parameter space.

Figure 5 summerizes the results for various values of λ_h. Each part of Figure 5 shows the original and the nonlinearly smoothed signal g and u, respectively, together with u_{c_ρ}. We have drawn the values used for λ_l and λ_h as lines of corresponding length (top-left), so that they can directly be compared to the image dimension. The zero-crossings of u_{c_ρ} are marked in the smoothed version of the signal. The following observations can be made (see Figure 5):

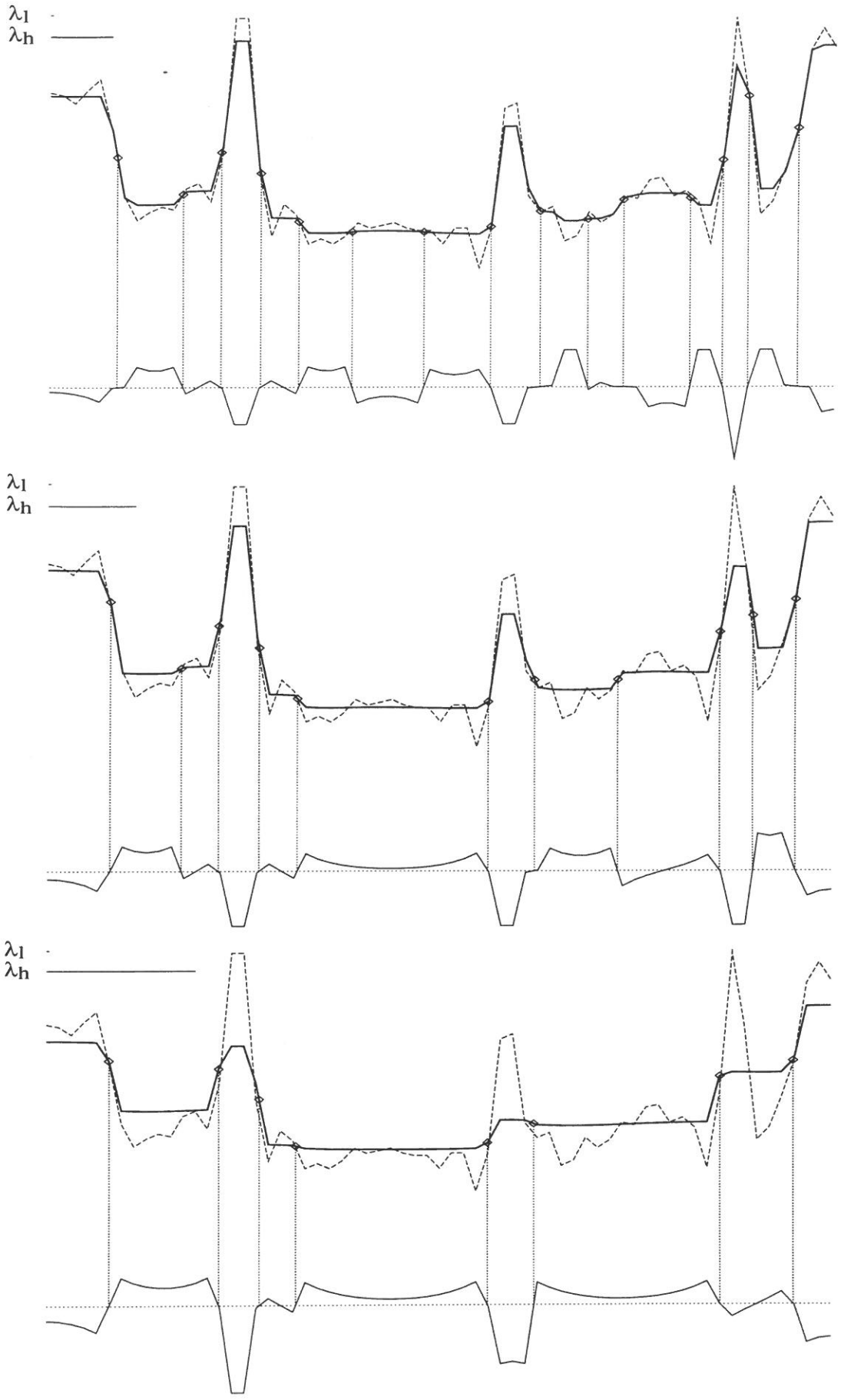

Figure 5: Numerical results of our segmentation method in parameter space (parameter $c_\rho = 0.2$, $\lambda_l = 0.2$, $\lambda_h = 5, 7, 12$) (see text)

- "Spurious" zero crossings, caused by subsequent steps in the same direction, for example, are not detected because they do not occur within low-smoothing regions.
- The curve u_{c_ρ} always comprises a small number of typical shapes. The environment of the spurious zero-crossings (up to the neighboring zero-crossings), for example, consists of three nearly linear segments. Other zero-crossings have at least on one side a "u"-formed shape, which can degenerate (in the case of a thin peak in the data) to a hill (or valley) with a flat plateau.
- Ramp-like transitions (relative to the current value of λ_h) show up as flat sections of u_{c_ρ} with a very low gradient.

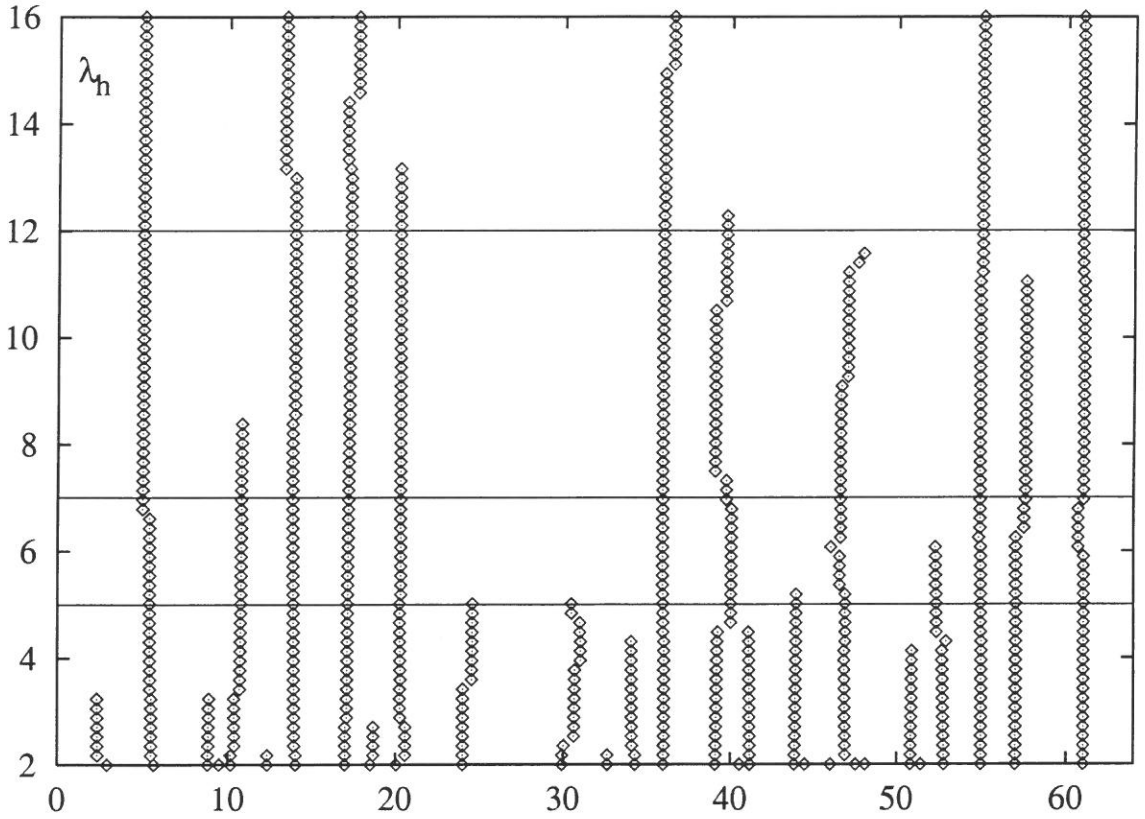

Figure 6: Zero-crossings of u_{c_ρ} over parameter-space $\{\lambda_h\}$. Parameter values: $c_\rho = 0.2$, $\lambda_l = 0.2$, $\lambda_h = 2 \ldots 16$. The horizontal lines mark the values of λ_h, which were used in figure 5

- Figure 5 showed that zero-crossings can only disappear if the value of λ_h increases. This corresponds to the interpretation of λ_h as a scale parameter. This is illustrated in Figure 6, where we plotted the positions of the zero-crossings over the parameter λ_h. Figure 6 reveals also that the positions of zero-crossings are remarkably stable within the parameter space. This is a significant improvement over purely linear scale-space methods. Slight shifts of zero-crossings over scale occur only at extended

ramp like transitions, where u_{c_ρ} has a very low gradient so that the zero-crossing is somewhat "weak".

Summarizing we conclude that the derivative u_{c_ρ} of nonlinearly diffused functions exhibits many useful features that systematically change over scale. We will explore in future work whether a symbolic description of real world data may be based on these features.

5 Conclusions and future work

In this contribution, we presented a novel scheme for detecting transitions in visual data. This scheme is based on an approach which has been recently developed by the authors where nonlinear diffusion is applied to visual data in a unique and numerically well-defined way. The parameter dependence of diffused functions has been investigated. Furthormore, it has been shown that signal transitions occur at points that are stable with respect to infinitesimal perturbations of a global parameter controlling the nonlinear diffusion process. The corresponding "tangent-vector" to the solution curve provides an interesting set of features that allows to characterize step and ramp like transitions and has been shown to be useful for analysing real world data over scale. The application of this ideas to higher-dimensional data will be explored in future work.

References

[1] J.P. Aubin. *Approximation of Elliptic Boundary-Value Problems.* Wiley&Sons, New York, 1972.

[2] M. Bertero, T. Poggio, and V. Torre. Ill-Posed Problems in Early Vision. *Proc. IEEE* **76**, 869–889, 1988.

[3] A. Blake and A. Zisserman. *Visual Reconstruction.* MIT Press, 1987.

[4] M. Carriero and A. Leaci. Existence Theorem for a Dirichlet Problem with Free Discontinuity Set. *Nonl. Anal., Theory, Methods & Appl.* **15** (7), 661–677, 1990.

[5] F. Catte, P.-L. Lions, J.-M. Morel, and T. Coll. Image Selective Smoothing and Edge Detection by Nonlinear Diffusion. *SIAM J. Numer. Anal.* **29** (1), 182–193, 1992.

[6] P.G. Ciarlet. *The Finite Element Method for Elliptic Problems.* North-Holland Publ. Comp., Amsterdam, 1978.

[7] E. De Giorgi, M. Carriero, and A. Leaci. Existence Theorems for a Minimum Problem with Free Discontinuity Set. *Arch. Rat. Mech. Anal.* **108**, 195–218, 1989.

[8] D. Geiger and A. Yuille. A Common Framework for Image Segmentation. *Int. J. of Comp. Vision* **6** (3), 227–243, 1991.

[9] S. Geman and D. Geman. Stochastic Relaxation, Gibbs Distributions, and the Bayesian Restoration of Images. *IEEE Trans. Patt. Anal. Mach. Intell.* **6** (6), 721–741, 1984.

[10] B.K.P. Horn and B.G. Schunck. Determining Optical Flow. *Artif. Intell.* **17**, 185–203, 1981.

[11] J. Hutchinson, C. Koch, J. Luo, and C. Mead. Computing Motion Using Analog and Binary Resistive Networks. *Computer* **21**, 52–63, 1988.

[12] K. Ikeuchi and B.K.P. Horn. Numerical Shape from Shading and Occluding Boundaries. *Artif. Intell.* **17**, 141–185, 1981.

[13] R. March. Visual Reconstruction with Discontinuities Using Variational Methods. *Image and Vis. Comp.* **10** (1), 30–38, 1992.

[14] J. Marroquin, S. Mitter, and T. Poggio. Probabilistic Solution of Ill-Posed Problems in Computational Vision. *J. Amer. Stat. Assoc.* **82**, 76–89, 1987.

[15] D. Mumford and J. Shah. Optimal approximations by piecewise smooth functions and associated variational problems. *Comm. Pure Appl. Math.* **42**, 577–685, 1989.

[16] P. Nesi. Variational Approach to Optical Flow Estimation managing Discontinuities. *Image and Vis. Comp.* **11** (7), 419–439, 1993.

[17] M. Nitzberg, D. Mumford, and T. Shiota. *Filtering, Segmentation and Depth*, volume 662 of *Lect. Not. Comp. Sci.* Springer-Verlag, Berlin, 1993.

[18] N. Nordström. Biased Anisotropic Diffusion - A Unified Regularization and Diffusion Approach to Edge Detection. *Image and Vis. Comp.* **8** (4), 318–327, 1990.

[19] P. Perona and J. Malik. Scale-Space and Edge-Detection. *IEEE Trans. Patt. Anal. Mach. Intell.* **12** (7), 629–639, 1990.

[20] T. Poggio and C. Koch. Ill-Posed Problems in Early Vision: From Computational Theory to Analogue Networks. *Proc. Roy. Soc. Lond. B* **226**, 303–323, 1985.

[21] T. Poggio, V. Torre, and C. Koch. Computationa Vision and Regularization Theory. *Nature* **317**, 314–319, 1985.

[22] C. Schnörr. Unique reconstruction of piecewise smooth images by minimizing strictly convex non-quadratic functionals. *J. of Math. Imag. Vision.* to appear.

[23] C. Schnörr and B. Neumann. Ein Ansatz zur effizienten und eindeutigen Rekonstruktion stückweise glatter Funktionen. In S. Fuchs and R. Hoffmann, editors, *Mustererkennung 1992, 14. DAGM-Symposium*, Dresden, September 1992, pages 411–416. Springer-Verlag.

[24] C. Schnörr and R. Sprengel. A nonlinear regularization approach to the integration of visual data. Technical Report FBI-HH-M-221/93, FB Informatik, Universität Hamburg, March 1993.

[25] H.R. Schwarz. *Numerische Mathematik.* B. G. Teubner Verlag, Stuttgart, 1986.

[26] J. Shah. Parameter Estimation, Multiscale Representation and Algorithms for Energy-Minimizing Segmentations. In *Proc. Int. Conf. Patt. Rec.*, Atlantic City, New Jersey, June 16-21 1990.

[27] R. Sprengel and C. Schnörr. Nichtlineare Diffusion zur Integration visueller Daten - Anwendung auf Kernspintomogramme. In S.J. Pöppl and H. Handles, editors, *Mustererkennung 1993, 15. DAGM-Symposium*, Lübeck, September 1993, pages 134–141. Springer-Verlag.

[28] D. Terzopoulos. Multilevel Computational Processes for Visual Surface Reconstruction. *Comp. Vis., Graph., and Imag. Proc.* **24**, 52–96, 1983.

[29] T. Wang, B. Mathur, A. Hsu, and C. Koch. Computing Optical Flow in the Primate Visual System: Linking Computational Theory with Perception and Physiologie. In R. Durbin, C. Miall, and G. Mitchison, editors, *The Computing Neuron*, pages 371–392. Addison-Wesley Publ. Comp., 1989.